

# Differential Elliptic Flow in 2 - 6 AGeV Au + Au Collisions: A New Constraint for the Nuclear Equation of State

P. Chung<sup>(1)</sup>, N. N. Ajitanand<sup>(1)</sup>, J. M. Alexander<sup>(1)</sup>, J. Ames<sup>†</sup>, M. Anderson<sup>(5)</sup>, D. Best<sup>(2)</sup>, F.P. Brady<sup>(5)</sup>, T. Case<sup>(2)</sup>,  
W. Caskey<sup>(5)</sup>, D. Cebra<sup>(5)</sup>, J.L. Chance<sup>(5)</sup>, B. Cole<sup>(11)</sup>, K. Crowe<sup>(2)</sup>, A. C. Das<sup>(3)</sup>, J.E. Draper<sup>(5)</sup>, M.L. Gilkes<sup>(1)</sup>,  
S. Gushue<sup>(1,9)</sup>, M. Heffner<sup>(5)</sup>, A.S. Hirsch<sup>(7)</sup>, E.L. Hjort<sup>(7)</sup>, W. Holzmann<sup>(1)</sup>, L. Huo<sup>(13)</sup>, M. Issah<sup>(1)</sup>, M. Justice<sup>(4)</sup>,  
M. Kaplan<sup>(8)</sup>, D. Keane<sup>(4)</sup>, J.C. Kintner<sup>(12)</sup>, J. Klay<sup>(5)</sup>, D. Krofcheck<sup>(10)</sup>, R. A. Lacey<sup>(1)</sup>, J. Lauret<sup>(1)</sup>, M.A. Lisa<sup>(3)</sup>,  
H. Liu<sup>(4)</sup>, Y.M. Liu<sup>(13)</sup>, J. Milan<sup>(1)</sup>, R. McGrath<sup>(1)</sup>, Z. Milosevich<sup>(8)</sup>, G. Odyniec<sup>(2)</sup>, D.L. Olson<sup>(2)</sup>, S. Panitkin<sup>(4)</sup>,  
C. Pinkenburg<sup>(9)</sup>, N.T. Porile<sup>(7)</sup>, G. Rai<sup>(2)</sup>, H.G. Ritter<sup>(2)</sup>, J.L. Romero<sup>(5)</sup>, R. Scharenberg<sup>(7)</sup>, L. Schroeder<sup>(2)</sup>,  
B. Srivastava<sup>(7)</sup>, N.T.B Stone<sup>(2)</sup>, T.J.M. Symons<sup>(2)</sup>, J. Whitfield<sup>(8)</sup>, T. Wienold<sup>(2)</sup>, R. Witt<sup>(4)</sup>, L. Wood<sup>(5)</sup>, and  
W.N. Zhang<sup>(13)</sup>

(E895 Collaboration )

P. Danielewicz<sup>(6)</sup>

<sup>(1)</sup>*Depts. of Chemistry and Physics, SUNY at Stony Brook, New York 11794-3400*

<sup>(2)</sup>*Lawrence Berkeley National Laboratory, Berkeley, California, 94720*

<sup>(3)</sup>*Ohio State University, Columbus, Ohio 43210*

<sup>(4)</sup>*Kent State University, Kent, Ohio 44242*

<sup>(5)</sup>*University of California, Davis, California, 95616*

<sup>6</sup>*Michigan State University, East Lansing MI 48824-1321 and  
Gesellschaft für Schwerionenforschung, Darmstadt, 64291 Germany*

<sup>(7)</sup>*Purdue University, West Lafayette, Indiana, 47907-1396*

<sup>(8)</sup>*Carnegie Mellon University, Pittsburgh, Pennsylvania 15213*

<sup>(9)</sup>*Brookhaven National Laboratory, Upton, New York 11973*

<sup>(10)</sup>*University of Auckland, Auckland, New Zealand*

<sup>(11)</sup>*Columbia University, New York, New York 10027*

<sup>(12)</sup>*St. Mary's College, Moraga, California 94575*

<sup>(13)</sup>*Harbin Institute of Technology, Harbin, 150001 P. R. China*

(October 24, 2018)

Proton elliptic flow is studied as a function of impact-parameter  $b$ , for two transverse momentum cuts in 2 - 6 AGeV Au + Au collisions. The elliptic flow shows an essentially linear dependence on  $b$  (for  $1.5 < b < 8$  fm) with a negative slope at 2 AGeV, a positive slope at 6 AGeV and a near zero slope at 4 AGeV. These dependencies serve as an important constraint for discriminating between various equations of state (EOS) for high density nuclear matter, and they provide important insights on the interplay between collision geometry and the expansion dynamics. Extensive comparisons of the measured and calculated differential flows provide further evidence for a softening of the EOS between 2 and 6 GeV/nucleon.

PACS 25.75.Ld

For several years now, the study of nuclear matter at high energy density has held the promise of providing valuable insights on the nuclear equation of state (EOS) and on the predicted phase transition to a quark-gluon plasma (QGP) [1–3]. At AGS energies of  $\sim 1 - 14$  AGeV, elliptic flow has emerged as an invaluable probe of high density nuclear matter [4–7]. This flow has been attributed to a delicate balance between (i) the ability of compressional pressure to effect a rapid transverse expansion of nuclear matter and (ii) the passage time for removal of the shadowing of participant hadrons by the projectile and target spectators [8]. If the passage time is long compared to the expansion time, spectator nucleons serve to block the path of participant hadrons emitted toward the reaction plane, and nuclear matter is squeezed-out perpendicular to this plane giving rise to negative

elliptic flow. For shorter passage times, the blocking of participant matter is significantly reduced and preferential in-plane emission or positive elliptic flow is favored because the geometry of the participant region exposes a larger surface area in the direction of the reaction plane. Thus, elliptic flow is predicted and found to be negative for beam energies  $\lesssim 4$  AGeV and positive for higher beam energies [6,7,9].

Recent theoretical studies of elliptic flow have suggested a sensitivity to the pressure at maximum compression [4,9,11] and thus to the stiffness of the EOS, and to possible QGP formation [6]. Despite this sensitivity, the commonly calculated patterns for elliptic flow very often do not constrain the EOS uniquely. This being the case, it is important to investigate additional experimental observables which may provide more stringent constraints

for the EOS. Here, we investigate the utility of differential elliptic flow measurements  $v_2(b)$  and  $v_2(b, p_T)$ , as possible constraints.

The measurements were performed at the Alternating Gradient Synchrotron (AGS) at the Brookhaven National Laboratory. Beams of  $^{197}\text{Au}$  at  $E_{Beam} = 2, 4,$  and  $6$  AGeV [10] were used to bombard a  $^{197}\text{Au}$  target of thickness calculated for a 3% interaction probability. Typical beam intensities resulted in  $\sim 10$  spills/min with  $\sim 10^3$  particles per spill. Charged reaction products were detected in the Time Projection Chamber (TPC) [12] of the E895 experimental setup. The TPC located in the MPS magnet (typically at 1.0 Tesla) provided good acceptance and charge resolution for charged particles  $-1 < Z < 6$  at all three beam energies. However, a unique mass resolution for  $Z = 1$  particles was not achieved for all rigidities. Data were taken in two experimental runs with a trigger which allowed for a wide range of impact-parameter selections as presented below.

Our flow analysis follows the now standard procedure [14] of using the second Fourier coefficient,  $v_2 = \langle \cos 2\phi \rangle$ , to measure the elliptic flow or asymmetry of the proton azimuthal distributions at mid rapidity ( $|y_{cm}| < 0.1$ ). This distribution can be expanded as

$$\frac{dN}{d\phi} \propto [1 + 2v_1 \cos(\phi) + 2v_2 \cos(2\phi)] , \quad (1)$$

where  $\phi$  represents the azimuthal angle of an emitted proton relative to the reaction plane. Near mid rapidity in a symmetric system  $v_1 \approx 0$ . The reference azimuthal angle  $\Phi_{plane}$  of the reaction plane is determined using [15] the vector  $\mathbf{Q}_i = \sum_{j \neq i}^n w(y_j) \mathbf{p}_{Tj} / p_{Tj}$ . Here,  $\mathbf{p}_{Tj}$  and  $y_j$  represent, respectively, the transverse momentum and the rapidity of baryon  $j$  ( $Z \leq 2$ ) in an event. The weight  $w(y_j)$  is assigned the value  $\langle p_x \rangle / \langle p_T \rangle$ , where  $p_x$  is the transverse momentum in the reaction plane [8]. The average  $\langle p_x \rangle$  is obtained from an earlier pass of an iterative procedure employed for each energy and impact-parameter selection.

The orientation of the impact-parameter vector follows azimuthal symmetry about the beam axis. Therefore, the azimuthal distribution of the determined reaction plane should be uniform or flat. We have established that deviations from this uniformity can be attributed to deficiencies in the acceptance of the TPC and have applied rapidity and multiplicity dependent corrections following Ref. [7]. The corrections were applied for each of several impact-parameter selections at each beam energy; they ensure the absence of spurious elliptic flow signals which might result from distortions in the reaction plane distribution. The dispersion of the reaction plane  $\langle |\phi_{12}| \rangle / 2$  was estimated for each impact-parameter  $b$  via the sub-event method [15]. Suffice to say, a reasonable resolution was observed over the entire range of energy and  $b$  studied. These estimates for the reaction plane dispersion serve as a basis for evaluating the dispersion corrections

summarized in Table 1; these corrections have been applied to the extracted flow values discussed below.

The event multiplicity of identified charged particles  $M_{filt}$  was used for centrality selection. That is, several multiplicity bins were selected in the range from 0.4 to 1.0  $M_{max}$  where  $M_{max}$  is the point in the charged particle multiplicity distribution where the height of the distribution has fallen to half its plateau value [16]. Impact-parameter estimates have also been made for these centrality selections, at each beam energy, via their respective fraction of the minimum bias cross section.

Figure 1 shows representative distributions in the azimuthal angle  $\phi$  obtained at the energies of 2, 4 and 6 AGeV for mid-rapidity ( $|y_{cm}^{(o)}| < 0.1$ ) protons. The panels from left to right represent the three beam energies, respectively, and from top to bottom the three impact-parameter ranges of  $0 \lesssim b \lesssim 3$ ,  $4 \lesssim b \lesssim 6$  and  $7 \lesssim b \lesssim 8$  fm. For visual clarity, a  $p_T$  cut has been applied to the distributions shown for both the 4 and 6 AGeV data, as indicated. Within each  $b$ -range in Fig. 1, the previously reported transition from negative to positive elliptic flow at  $\approx 4$  AGeV [7] is clearly seen. That is, the elliptic flow is negative at 2 AGeV, positive at 6 AGeV and essentially zero at 4 AGeV. An apparent increase of the anisotropy of the distributions with increasing  $b$  can also be discerned for the 2 and 6 AGeV data shown in Fig. 1. We attribute this trend to an interplay of the changing geometry with the expansion of excited participant matter as discussed below.

Figure 2 shows the  $v_2$  coefficients for the full  $p_T$  range, as a function of  $b$  for data (filled stars) obtained at 2, 4, and 6 AGeV in the three panels, respectively. These coefficients have been obtained by evaluating the  $\langle \cos 2\phi \rangle$  for each azimuthal distribution obtained for a given impact-parameter at each beam energy. A correction has been applied to some of these coefficients to account for biases resulting from (i) low  $p_T$  acceptance losses in the TPC for the 2, 4, and 6 AGeV beams, (ii) high  $p_T$  acceptance losses in the TPC for the 2 AGeV beam, and (iii)  $\pi^+$  contamination of the proton sample at 4 and 6 AGeV [17,7]. A procedure for effecting these corrections has been detailed in Ref. [7]. That is, we first plotted the observed Fourier coefficient  $\langle \cos 2\phi' \rangle$  vs.  $p_T$  with  $p_T$  thresholds which allowed clean particle separation ( $p_T \sim 1$  GeV/c). We then extracted the coefficients for the quadratic dependence of  $\langle \cos 2\phi' \rangle$  on  $p_T$ . These quadratic fits are restricted by the requirement that  $\langle \cos 2\phi' \rangle = 0$  for  $p_T = 0$ . Next, we corrected the proton  $p_T$  distributions for possible high and low  $p_T$  losses. A weighted average (relative number of protons in a  $p_T$  bin times the  $\langle \cos 2\phi' \rangle$  for that bin) was then performed to obtain  $\langle \cos 2\phi' \rangle$  for each beam energy. The corrections which result from this procedure are  $\sim 5\%$  for the 4 and 6 AGeV beams and  $\sim 15\%$  for the 2 AGeV beam. Subsequent to these evaluations, the  $v_2$  values were corrected for reaction plane dispersion

using the procedures detailed in Refs. [7,14,15,18].

The  $v_2$  values represented by filled stars in Fig. 2 indicate an essentially linear dependence on impact parameter. The slope of this dependence is clearly negative and positive for the 2 and 6 AGeV data, respectively. By contrast, an essentially flat dependence is observed for the 4 AGeV data suggesting that the beam energy at which the elliptic flow changes sign is not very sensitive to  $b$  for  $0 \lesssim b \lesssim 8$  fm. The approximately linear dependence exhibited by the data can be understood in terms of the collision geometry and the development of transverse expansion within the participant matter. At 2 AGeV an expansion perpendicular to the reaction plane develops over the characteristic time of  $d/c_s$  while the spectators are present. Here,  $c_s = \sqrt{\partial p / \partial e}$  represents the speed of sound for a given pressure  $p$ , and energy density  $e$ , and  $d$  is the perpendicular distance from the center of the participant region to the surface. The spectator passage time (estimated in sharp cut-off geometry) first increases and then remains essentially constant as  $b$  increases over the range of interest. On the other hand, the expansion time decreases with increasing  $b$  due to a decrease in  $d$ . It is this decrease in the expansion time coupled with an essentially constant passage time, which provides the driving force for more matter to escape the interaction region as  $b$  is increased i.e. an increase in “squeeze-out” with  $b$ . The magnitude of the “squeeze-out” follows an approximately linear dependence because  $d$  is roughly proportional to  $1/b$  for the Au + Au impact parameter range 1 - 8 fm.

At 6 AGeV the spectator passage time is very short compared to the expansion time and preferential in-plane emission dominates. In this case, however, the linear increase of  $v_2$  with increasing impact parameter is strongly influenced by the initial spatial asymmetry of the nuclei overlap region or participant matter. This asymmetry is commonly characterized in terms of the width  $L_x$  and height  $L_y$  of the overlapping region via  $\alpha_s = (L_y - L_x)/(L_y + L_x)$  [9] and can be shown to be nearly linearly proportional to the impact parameter for medium  $b$  values. The essentially flat dependence of  $v_2$  observed at 4 AGeV suggests that, at the transition energy, the reduction in the expansion time [in competition with the spectator passage time] with increasing  $b$ , is compensated for by the (later) increased in-plane-emission from the preserved initial spatial asymmetry.

The solid circles, open squares and solid triangles shown in Figs. 2, represent results from calculations with a recent version of the Boltzmann Equation Model BEM [6] which assumes a soft ( $K = 210$  MeV), a stiff ( $K = 380$  MeV) and an intermediate ( $K = 300$  MeV) EOS respectively. The calculations include momentum dependent forces [19]. A comparison of the calculated  $v_2$  values indicate sizeable differences between the predictions for a stiff and a soft EOS for all three beam ener-

gies. For both 2 and 4 AGeV this distinction increases with increasing impact parameter indicating that the impact parameter dependence of elliptic flow lends a new and important constraint for the EOS. At 2 AGeV, the  $v_2$  values for the stiff EOS show good agreement, both in magnitude and trend, with the experimental data. At 4 AGeV the measured  $v_2$  values lie between the calculated result for a stiff and a soft EOS, and appear to be in better overall agreement with an intermediate form of the EOS. At 6 AGeV the data is less compatible with a stiff EOS, but does not allow a clear distinction between the soft and the intermediate ( $K = 300$  MeV) EOS. The results of these comparisons can be taken as being suggestive of a softening of the EOS as previously reported in Ref. [7]. However, it is interesting to investigate whether or not the differential flow measurement  $v_2(b, p_T)$  provides further constraints. This line is pursued below.

Figs. 3 compares experimental (stars) and calculated (circles, triangles and squares) differential elliptic flow  $v_2(b, p_T)$  for 2, 4 and 6 AGeV as indicated. At each beam energy, the BEM calculations have been carried out for the same  $p_T$  and  $b$  selections applied to the data. Fig. 3 indicates good agreement between the data and the calculated results for a stiff EOS at 2 AGeV. At 4 AGeV the data again shows better overall agreement with the intermediate and soft EOS. At 6 AGeV the comparison indicates quite good agreement (both in magnitude and trend) between the data and the results from the calculations which assume a soft EOS. The latter agreement is in contrast to the results obtained from the comparison made in Fig. 2, and clearly indicates that the differential flow  $v_2(b, p_T)$ , does indeed provide an additional constraint for making a relatively clear distinction between the different EOS's at 6 AGeV.

To summarize, we have studied differential proton elliptic flow in 2 - 6 AGeV Au + Au collisions. The elliptic flow shows an essentially linear dependence on  $b$ , in the range  $1.5 \lesssim b \lesssim 8$  fm, with a negative slope at 2 AGeV, approximately zero slope at 4 AGeV, and a positive slope at 6 AGeV. This dependence can be understood in terms of (a) the relationship between the collision geometry, (b) the relative magnitude of the time for development of the transverse expansion, and (c) the passage time for removal of the shadowing of participant hadrons by the projectile and target spectators. Detailed comparisons between the measured differential elliptic flow  $v_2(b, p_T)$ , and  $v_2(b)$ , and the results obtained from a relativistic Boltzmann-equation calculation not only suggest a softening of the EOS but also indicate that differential flow measurements provide very important constraints for the determination of the EOS of high density nuclear matter.

## ACKNOWLEDGMENTS

This work was supported in part by the U.S. Department of Energy under grants DE-FG02-87ER40331.A008, DE-FG02-89ER40531, DE-FG02-88ER40408, DE-FG02-87ER40324, and contract DE-AC03-76SF00098; by the US National Science Foundation under Grants No. PHY-98-04672, PHY-9722653, PHY-0070818, PHY-9601271, and PHY-9225096; and by the University of Auckland Research Committee, NZ/USA Cooperative Science Programme CSP 95/33.

- 
- [1] H. Stoecker and W. Greiner, Phys. Rep. 137, 277, (1986).
  - [2] *Quark Matter '96, Proc. 12th Int. Conf. on Ultra-Relativistic Nucleus-Nucleus Collisions, Heidelberg, Germany, 1996*, ed. P. Braun-Munzinger *et al.*, Nucl. Phys. A610, 1c-572c (1996).
  - [3] W. Reisdorf and H. G. Ritter, Annu. Rev. Nucl. Part. Sci. 47, 663 (1997).
  - [4] H. Sorge, Phys. Rev. Lett. 78, 2309 (1997).
  - [5] J. Barrette *et al.*, Phys. Rev. C 56, 3254 (1997).
  - [6] P. Danielewicz *et al.*, Phys. Rev. Lett. 81, 2438 (1998).
  - [7] C. Pinkenburg *et al.*, Phys. Rev. Lett. 83, 1295 (1999).
  - [8] P. Danielewicz, Phys. Rev. C 51, 716 (1995).
  - [9] J.-Y. Ollitrault, Phys. Rev. D 46, 229 (1992).
  - [10] Actual beam energies are 1.85, 3.9 and 5.9 AGeV respectively.
  - [11] J.-Y. Ollitrault, Phys. Rev. D 48, 1132 (1993).
  - [12] G. Rai, IEEE Trans. Nucl. Sci. 37, 56 (1990).
  - [13] G. Bauer, NIM A 386, 249 (1997).
  - [14] M. Demoullins *et al.*, Phys. Lett. B 241, 476 (1990); M. Demoullins, Ph. D. Thesis, University Paris Sud, 1989 (Report CEA-N-2628, CEN Saclay, 1990).
  - [15] P. Danielewicz and G. Odyniec, Phys. Lett. B 157, 146 (1985).
  - [16] H. H. Gutbrod, Rep. Prog. Phys. 52, 1267 (1989).
  - [17] Unique separation of  $\pi^+$  and protons was not achieved for all rigidities at all beam energies.
  - [18] J.-Y. Ollitrault, nucl-ex/9711003 v2.
  - [19] P. Danielewicz, Nucl.Phys.A 673, 375 (2000).

b range (fm)	Dispersion Correction Factor		
	2 AGeV	4 AGeV	6 AGeV
$0 < b < 3$	1.71	2.64	4.65
$4 < b < 6$	1.22	1.59	2.47
$7 < b < 8$	1.26	1.99	2.86

Table 1: Correction factors for reaction plane dispersion for several impact parameter ranges for the 2, 4 and 6 AGeV beam energies.

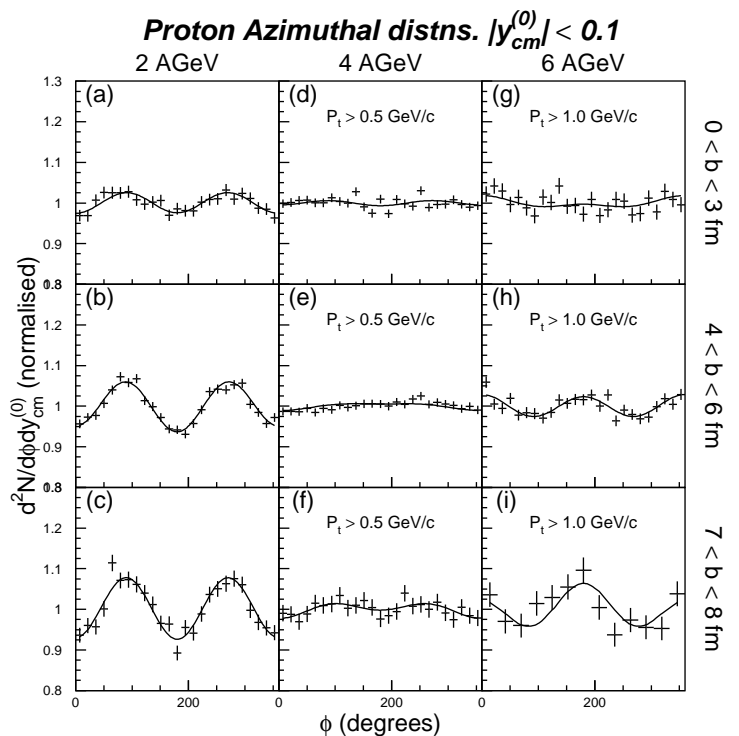


FIG. 1. Measured azimuthal distributions for Au + Au collisions. Distributions are shown for the impact-parameter ranges of  $0 \leq b \leq 3$  fm,  $4 \leq b \leq 6$  fm and  $7 \leq b \leq 8$  fm and the beam energies of 2 (a, b, c), 4 (d, e, f) and 6 (g, h, i) AGeV, as indicated. The solid lines are drawn to guide the eye.

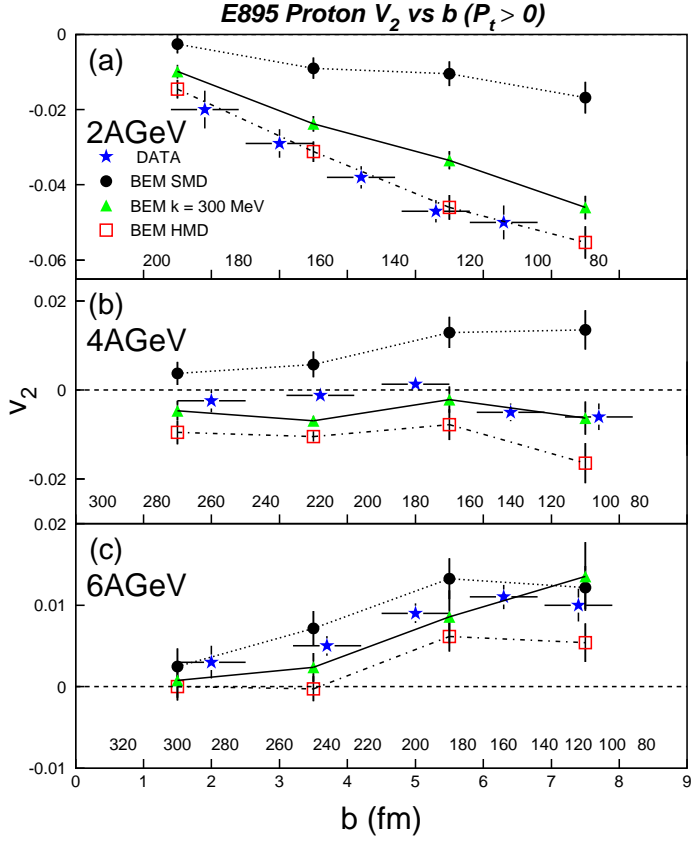


FIG. 2.  $v_2$  as a function of  $b$  ( $p_T > 0$ ) for 2 (a), 4 (b) and 6 (c) AGeV Au + Au collisions. Experimental values are indicated by the filled stars. The open squares, full circles and solid triangles represent  $v_2$  values from BEM calculations with a stiff ( $K = 380$  MeV), a soft ( $K = 210$  MeV) and an intermediate ( $K = 300$  MeV) momentum-dependent EOS respectively. The identified charged particle multiplicity  $M_{fillt}$ , is also indicated for several values of  $b$ . The solid, dotted and dashed-dotted lines serve to guide the eye only.

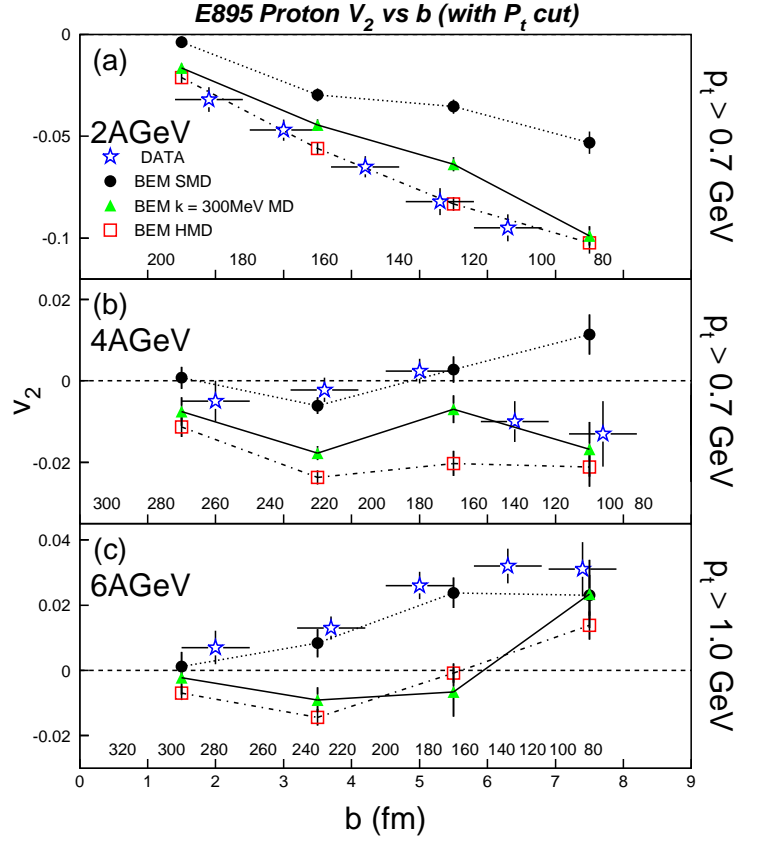


FIG. 3. Same as Figs.2 except that a  $p_T > 0.7$  GeV cut has been applied on the data and calculations at 2 and 4 AGeV and a  $p_T > 1.0$  GeV cut has been applied at 6 AGeV.